Chapter 2

Applications of Mach-Zehnder Interferometry to Studies on Local Deformation of Polymers Under Photocuring

Dan-Thuy Van-Pham, Minh-Tri Nguyen,
Hideyuki Nakanishi, Tomohisa Norisuye and
Qui Tran-Cong-Miyata

Additional information is available at the end of the chapter

http://dx.doi.org/10.5772/64611

Abstract

A Mach-Zehnder interferometer (MZI) was built and modified to in situ monitor the deformation of polymers during the photocuring process. In this review, the working principle and method of operation of this MZI were explained together with the method of data analysis. As the examples for the utilization of this modified MZI, measurements of the deformation induced by photopolymerization was demonstrated for three different types of samples: homopolymer in the bulk state, miscible polymer blends and phase-separated polymer blends. Finally, a concluding remark is provided for the usage of MZI in polymer research.

Keywords: Mach-Zehnder interferometry, light scattering, poly(ethyl acrylate), poly(vinyl methyl ether), polystyrene, polymer blends, concentration fluctuations, phase separation, glass transition temperature, photo-cross-linking (photocuring), photodimerization, shrinkage, swelling

1. Introduction

Mach-Zehnder interferometry (MZI) was invented by Ludwig Zehnder in 1891 [1] and was subsequently refined by Ludwig Mach in the year after [2]. The techniques were invented taking advantages of the interference phenomena of light to measure the phase difference between the two light beams in which one is varied by the presence of a sample. As illustrated in **Figure 1**, the basic structure of the interferometry is composed of one beam splitter (half mirror) and two

reflecting mirrors. The coherent light beam from a laser after collimation was divided into two beams: the reference beam and the test beam on which the sample is interposed. These two beams serve as two arms, the reference and the test arms of the interferometry. The presence of an object on the test arm will result in the difference in optical path length, thereby changing the interference pattern of the laser at the half mirror [HM2]. The fringe patterns can be monitored and recorded either along the direction of the reference beam or the test beam. Compared to other interferometers like Michelson, the separation of the two arms of MZI can provide a wide application due to large and freely accessible working space though the optical alignment is relatively difficult. Taking advantage of this spacious working place, MZI has been utilized for various experiments: electron interferometer functioning in high magnetic field [3], flow visualization and flow measurements [4], for sensing applications [5]. Furthermore, optofluidic Mach-Zehnder interferometer for sensitive, label-free measurements of refractive index of fluids was also developed [6]. The unique structure of Mach-Zehnder has also been utilized for optical communication as a modulator [7]. On the other hand, a lot of efforts have been made to fabricate microscale optical systems including Mach-Zehnder interferometer modulators using polymeric materials [8, 9]. In this chapter, we focus on studies on the local deformation in polymeric systems undergoing photocuring by ultraviolet (UV) light. Since the polymer mixture undergoes transition from liquid to solid by the reaction and at the same time phase separation takes place, the deformation (shrinkage and/or swelling) would affect the phase separation process and the resulting morphology. Mach-Zehnder interferometry would be useful to monitor the extent of deformation in the nanometer scales during the reaction.

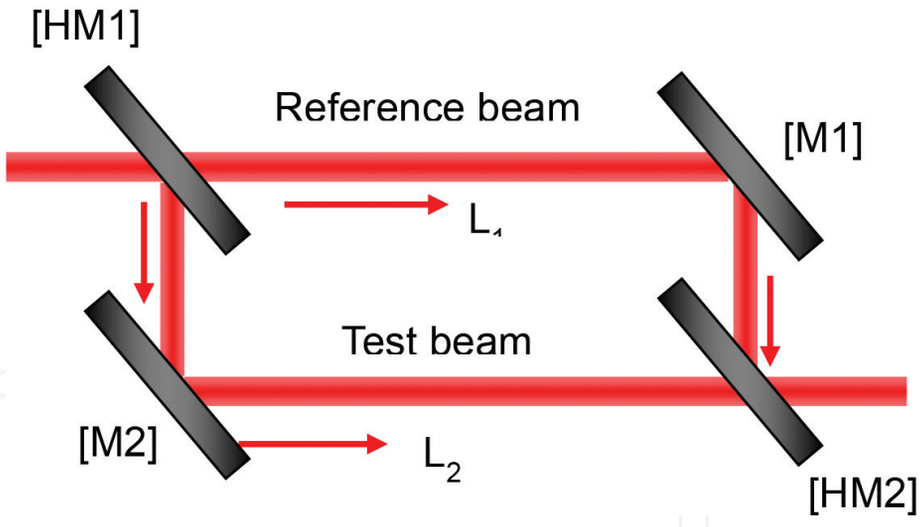

Figure 1. Basic unit of Mach-Zehnder interferometry (MZI).

2. Instrumentation and data analysis

The block diagram of the MZI used in our experiments is illustrated in **Figure 2**.

The details are described in a previous publication [10]. Briefly, a coherent 632.8 nm light beam from a He-Ne laser is passed through a Glan-Thompson prism and is converted into

http://dx.doi.org/10.5772/64611

vertically polarized light. The polarized light beam was collimated by using collimating lens before entering the basic unit of the Mach-Zehnder interferometer. After passing the half mirror [HM1], incident light was divided into two beams, forming the reference arm and the test arm of the MZI. A sample was interposed on the test arm and was half hidden by a movable mask to produce the reference part on the sample. The deformation of the sample under curing is obtained from the variation of the part irradiated with UV light compared to the part hidden by a mask on the same sample. In order to observe the deformation caused by the curing reaction, the sample was submitted to the sequence of *masking-irradiating-mask removing-recording*. Movement of this mask is controlled with the precision of a micrometer. Details of the operation are provided in [10]. These two laser beams encounter with each other at the half mirror [HM2] to produce interference patterns which were recorded on a charge-coupled device (CCD) camera. The data were subsequently analyzed using a computer.

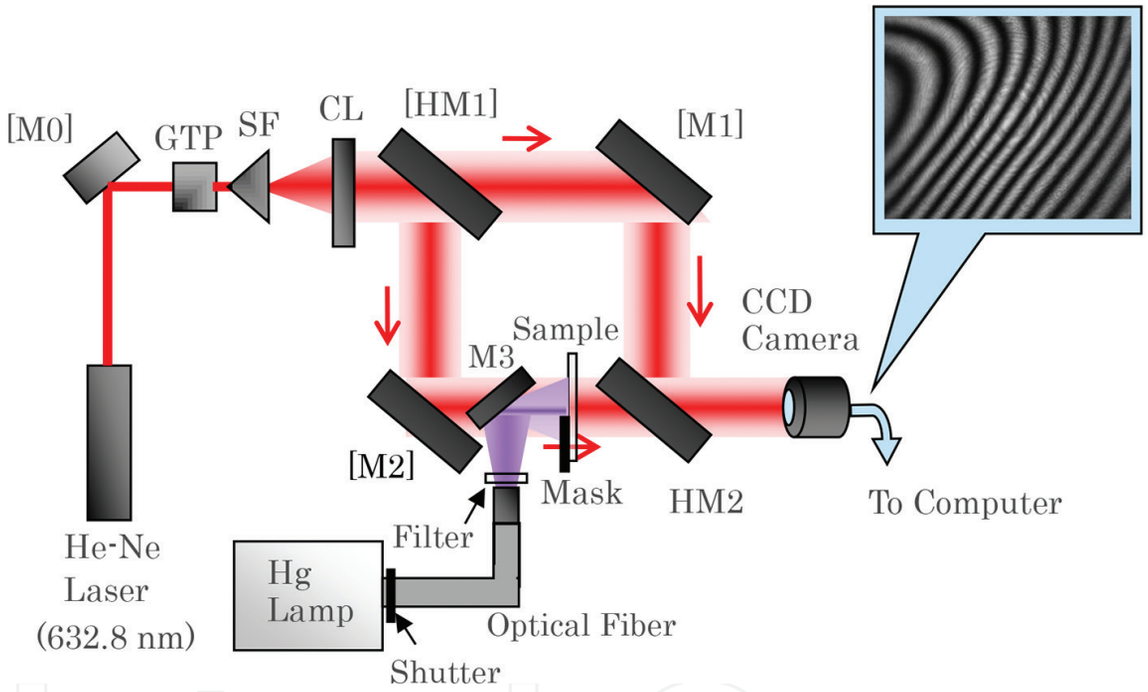

Figure 2. The block diagram of the Mach-Zehnder interferometer (MZI) used in this study for in situ monitoring the deformation induced by photocuring polymers. M, reflecting mirror; HM, half-mirror; GTP, Glan-Thompson prism; SF, spatial filter; CL, collimating lens.

2.1. Basic theory of light interference phenomena

Two monochromatic planar waves E_1 and E_2 traveling along the two arms of the Mach-Zehnder interferometer can be expressed by the following wave equation in complex form:

$$E_1 = E_{01} \exp(i\phi_1) \tag{1}$$

$$E_2 = E_{02} \exp(i\phi_2) \tag{2}$$

Here E and ϕ represent respectively the amplitudes and the phases of the two waves and i is the imaginary number.

The phase of these two waves can be written as

$$\phi_1 = k\, n_0\, L_1 \tag{3}$$

$$\phi_2 = k\, n_0\, L_2 \tag{4}$$

where k and n_0 are respectively the wavenumber of the incident light and the refractive index of the sample before curing. L_1 and L_2 are respectively the path length of light traveling along the reference and the test arms. The phase difference between the two beams can be expressed by

$$\Delta\phi = \left(\phi_2 - \phi_1\right) = k\left(L_2 - L_1\right) \tag{5}$$

where n_0, the refractive index of air was set equal unity. If the length of two arms is set equal $L_1 = L_2$, $\Delta\phi = 0$. There is no interference for this particular case. In the presence of a sample with refractive index n and the thickness d interposed on the test arm, the phase of the wave traveling along this direction becomes

$$\phi_2 = k\,.\,n_0\,.\left(L_2 - d\right) + k\,.\,n\,.\,d \tag{6}$$

The phase difference in the presence of the sample becomes:

$$\Delta\phi = \left(\phi_2 - \phi_1\right) = k(n-1)d + k\left(L_2 - L_1\right) \tag{7}$$

For the case $L_1 = L_2$, the phase difference becomes

$$\Delta\phi = k(n-1)\, d \tag{8}$$

Therefore, the optical path length (OPL) of the sample *before* irradiation is

$$\mathrm{OPL}_{\mathrm{before}} = \frac{\Delta\phi_{\mathrm{before}}}{k} = (n-1)\, d \tag{9}$$

In general, both the refractive index and the thickness of the sample are varied by the reaction:

$$\mathrm{OPL}_{\mathrm{after}} = \left(\frac{\Delta\phi_{\mathrm{after}}}{k}\right) = (n + \Delta n)(d + \Delta d) - 1.(d + \Delta d) \tag{10}$$

Since both Δn and Δd are small, $(\Delta n\,.\,\Delta d)$ can be neglected, leading to the final result

$$\text{OPLD} = \left(\text{OPL}_{\text{after}} - \text{OPL}_{\text{before}}\right) = \Delta d \,.\, (n-1) + \Delta n \,.\, d \tag{11}$$

For the case, the change in refractive index is negligible, $\Delta n \cong 0$, the optical path length can be approximately expressed as

$$\text{OPLD} \cong \Delta d \,.\, (n-1) \tag{12}$$

If the initial thickness (before curing) of the sample is d_0, from definition, the deformation ε (either shrinkage or swelling) is given by the below equation:

$$\varepsilon = \frac{\Delta d}{d_0} = \frac{\text{OPLD}}{(n-1)\ d_0} = \frac{\text{OPLD}}{(n-1)\ d_0} \tag{13}$$

The OPLD on the left-hand side can be obtained from MZI experiments. Therefore, if the change in refractive index Δn before and after the curing reaction can be directly measured using some instrument like prism coupler [11], the change in the sample thickness Δd can be obtained.

2.2. Data analysis

The interference patterns obtained for a polymer film under in situ photocuring on the test arm of the MZI are recorded by using a CCD camera. Though the laser beam was passed through the spatial filter to select the best part of the beam and was subsequently collimated before entering the MZI unit, the interference patterns are slightly affected by the spatial distribution of the laser intensity. This effect can be removed by performing some correction assuming that the shape of the laser beam is Gaussian [10].

The interferograms obtained before and after this correction for the intensity distribution of a He–Ne laser (NEC, 1 mW) in the case a polystyrene/poly(vinyl methyl ether) PS/PVME (30/70) blend was used as sample are, respectively, illustrated in **Figures 3** and **4**. To reduce noise, the 2D data (480 pixel × 640 pixel) were divided into 48 horizontal strips with the dimension (10 pixel × 640 pixel) for each strip. Data along the *y*-axis for each strip were then averaged to provide 1D data as shown in **Figure 3(a)**.

In general, the real part of the intensity of an interferogram is a periodic function of distance and can be expressed in 1D as follows:

$$I(x) = a(x)\cos\left[\phi(x)\right] \tag{14}$$

where $a(x)$ and $\phi(x)$ are the amplitude and phase of the signal, respectively.

The imaginary part $J(x)$ of the intensity can be calculated by using Hilbert transform [10, 12]. From these calculations, the amplitude $a(x)$ and the phase $[\phi(x)]$ are obtained:

$$a(x) = \sqrt{I^2(x) + J^2(x)} \tag{15}$$

$$\text{and } \varphi(x) = \tan^{-1}\left(\frac{J(x)}{I(x)}\right) \tag{16}$$

Finally, the OPLD can be obtained for the left-hand side of Eq. (12).

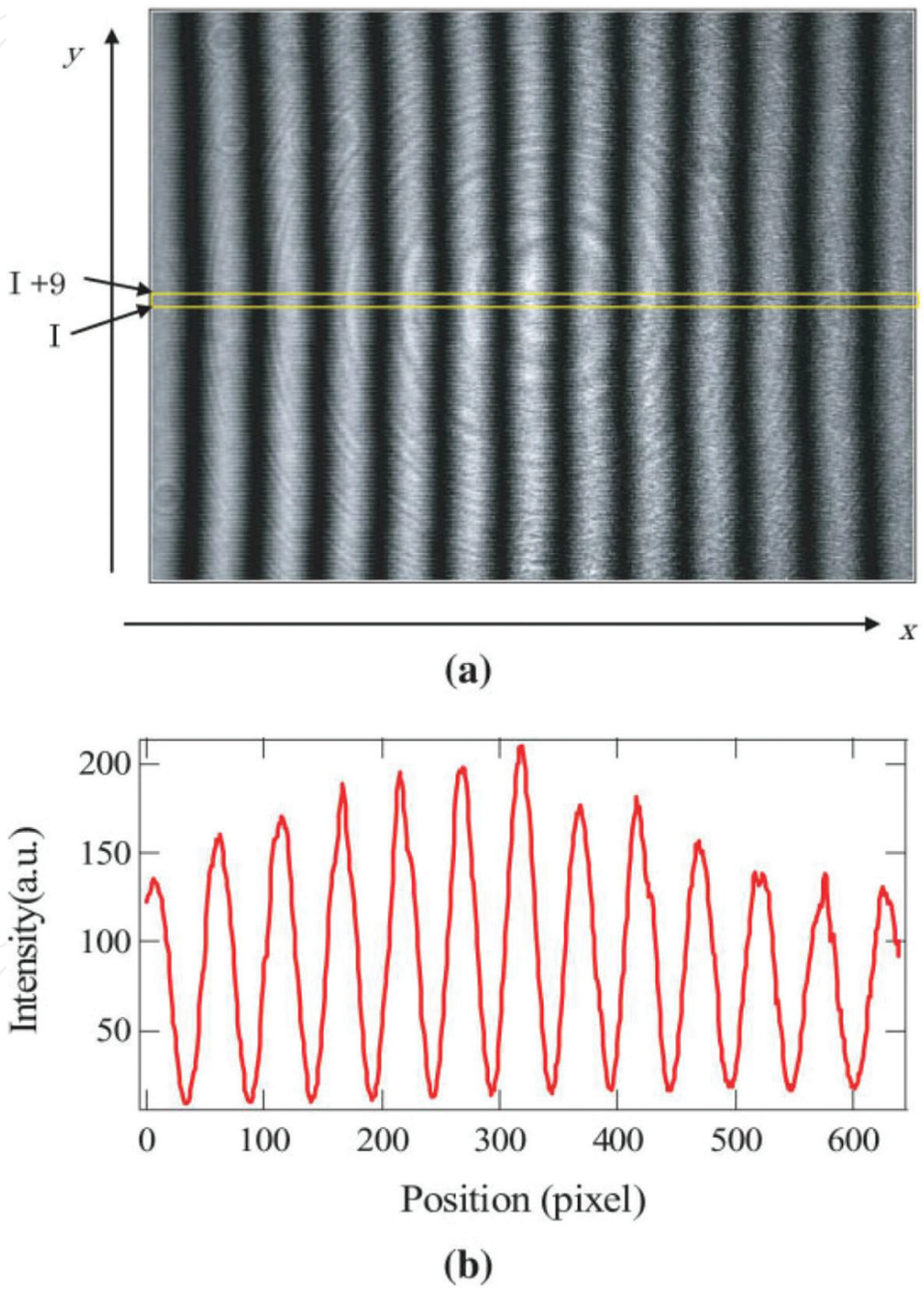

Figure 3. (a) Interferogram obtained at 20°C for a PSA/PVME (30/70) blend; (b) 1D data obtained by averaging along the *y* direction for each 10 pixels indicated by the two arrows in (a). The peripheral of the intensity distribution in (b) is affected by the Gaussian beam.

http://dx.doi.org/10.5772/64611

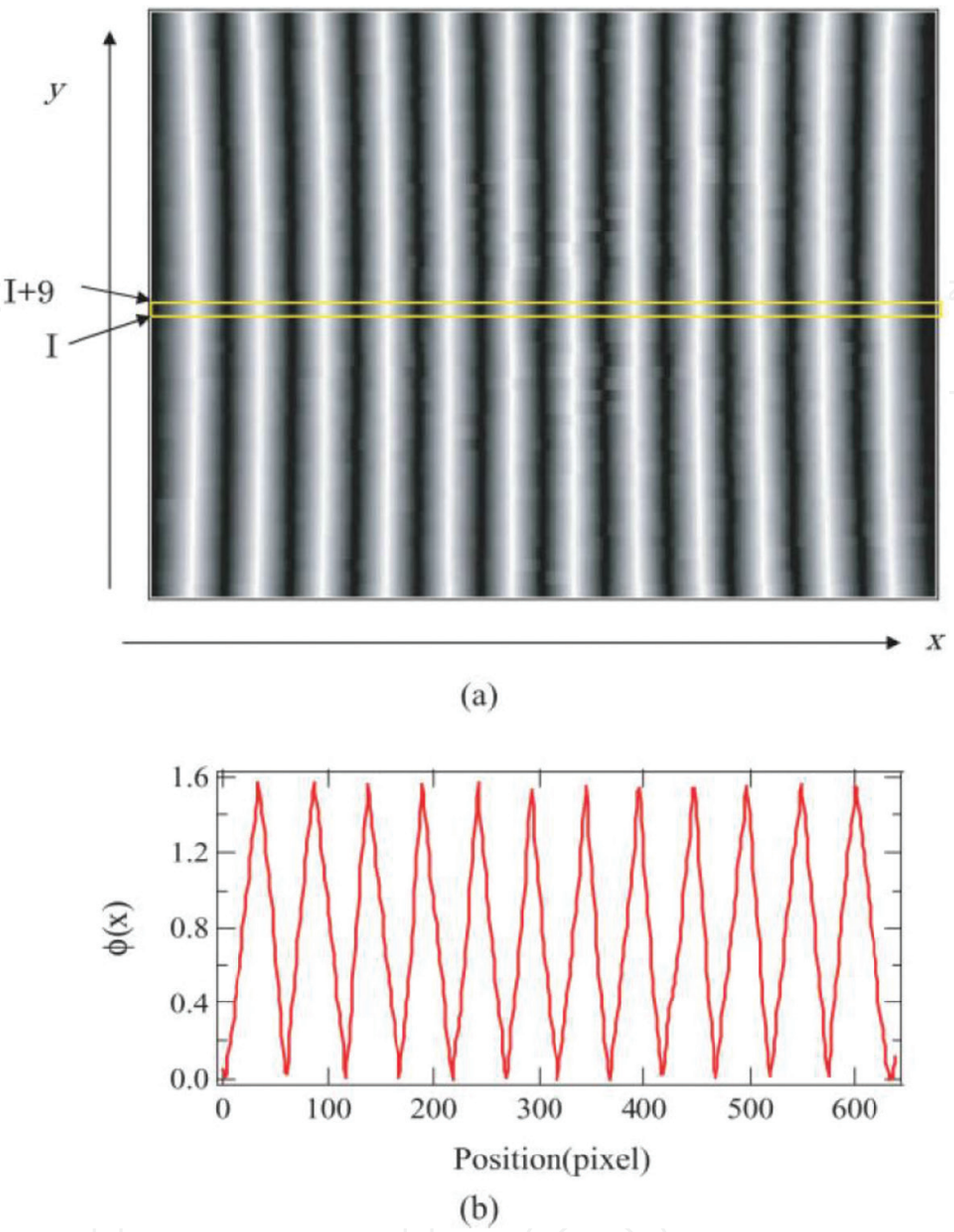

Figure 4. (a) The interferogram shown in **Figure 4** after the Hilbert transformation; (b) the 1D intensity distribution after averaging along the *y*-axis as described for **Figure 3**.

3. Samples

Polymers used in this study are the derivatives of poly(ethyl acrylate) (PEA), polystyrene (PS) and poly(vinyl methyl ether) (PVME). The mixture of PS and PVME exhibits miscibility at room temperature, providing a system for studying the effects of shrinkage on phase separation of polymer blends. All polymers used here have molecular weight larger than 100.000 and the molecular weight distribution around 2.0. The details of chemical synthesis and sample characterization are described in previous publications [13, 14].

Samples for MZI studies were obtained by solvent casting method and were dried under vacuum at least one night. All the samples PS/PVME mixtures with the dimension (20 mm × 20 mm × 10 μm) were annealed under vacuum over 2 h at temperature above the glass transition temperature (T_g) of the blend to erase the thermal history of the preparation process.

3.1. Photodimerization of anthracene as a photocuring reaction

To photo-cross-link a polymer with UV irradiation, photosensitive anthracene was chemically labeled on a given polymer by copolymerizing its monomer with a photoreactive monomer by copolymerization. By doing so, photoreactive anthracene moieties were introduced into the polymer component under examination. The labeling content of anthracene can be adjusted by varying the ingredients of the coupling reactions. Upon irradiation with 365 nm UV light, anthracene undergoes photodimerization as illustrated in **Figure 5** for the case of PEA chains.

3.2. In situ observation of the deformation kinetics in homopolymers undergoing photocuring and relation to physical aging of the photocured polymer

Poly(ethyl acrylate) (PEA, $M_w = 1.6 \times 10^5$, $M_w/M_n = 2.2$) was prepared by conventional free radical polymerization. To be able to cure PEA with UV irradiation, the PEA was chemically labeled with anthracene which served as a cross-linker of the PEA chains as illustrated in **Figure 5**. Upon irradiation with 365 nm UV light, the anthracene moieties labeled on PEA undergoing photodimerization, generating PEA networks in the sample. As a consequence, the sample gradually approaches the glassy state and exhibits shrinkage due to the liquid→solid transition. However, this shrinkage in this particular case is fairly small and could not be observed via monitoring the change in the sample thickness by laser-scanning confocal microscopy as in the case of photopolymerization [15]. As the cross-link density in the sample reaches a critical value, PEA enters the glassy state. Depending on the rate at which PEA enters the glassy state, physical aging [16] could occur. This feature can be observed via the irradiation intensity dependence of the shrinkage associated with irradiation time as shown in **Figure 6**. Here, the deformation ε which was calculated from the OPLD data given in Eq. (13) for the case of negligible change in refractive index is plotted versus irradiation time and elapse time. It is worth noting that the physical aging phenomena are evidenced by the continuation of shrinkage after stopping irradiation. These results suggest that the sample with the cross-link density $\gamma \sim 2$ already enters the glassy state during irradiation, exhibiting the physical aging phenomena. Compared to the result obtained at low light intensity, it was found that the physical aging of photo-cross-linked PEA sample emerges at the cross-link density $\gamma \geq 2$ junctions /chain. This aging process becomes stronger under irradiation with higher light intensity. From the plot of normalized shrinkage ($\varepsilon/\varepsilon_{max}$) vs. non-dimensionalized elapse time defined as ($t_e \,.\, k_a$) where t_e is the elapse time and k_a is the characteristic time of the aging process, it was found that all the aging data obtained with a constant irradiation intensity can be expressed by a master curve [17].

3.3. Local deformation of miscible polymer blends under photocuring and relation to physical aging

Mach-Zehnder interferometry was also utilized to detect the local deformation in miscible polymer blends polystyrene derivative (PS) and poly(vinyl methyl ether) (PVME). The curing

http://dx.doi.org/10.5772/64611

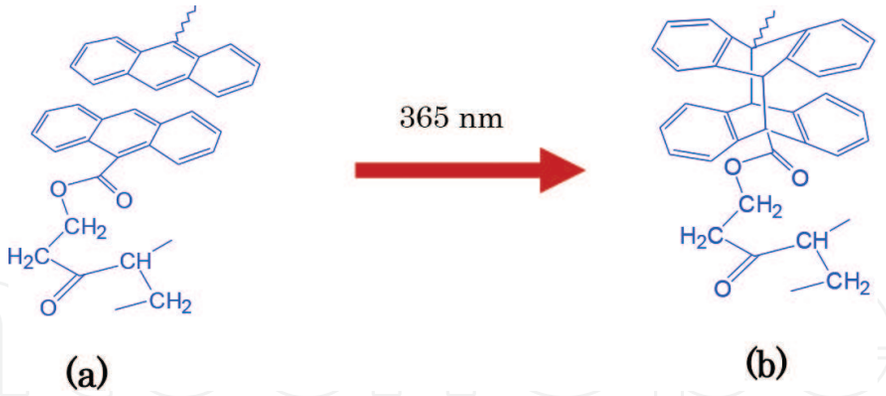

Figure 5. Photodimerization of anthracene chemically labeled on poly(ethyl acrylate): (a) before photodimerization, (b) after photodimerization with the formation of photodimer between two segments of PEA.

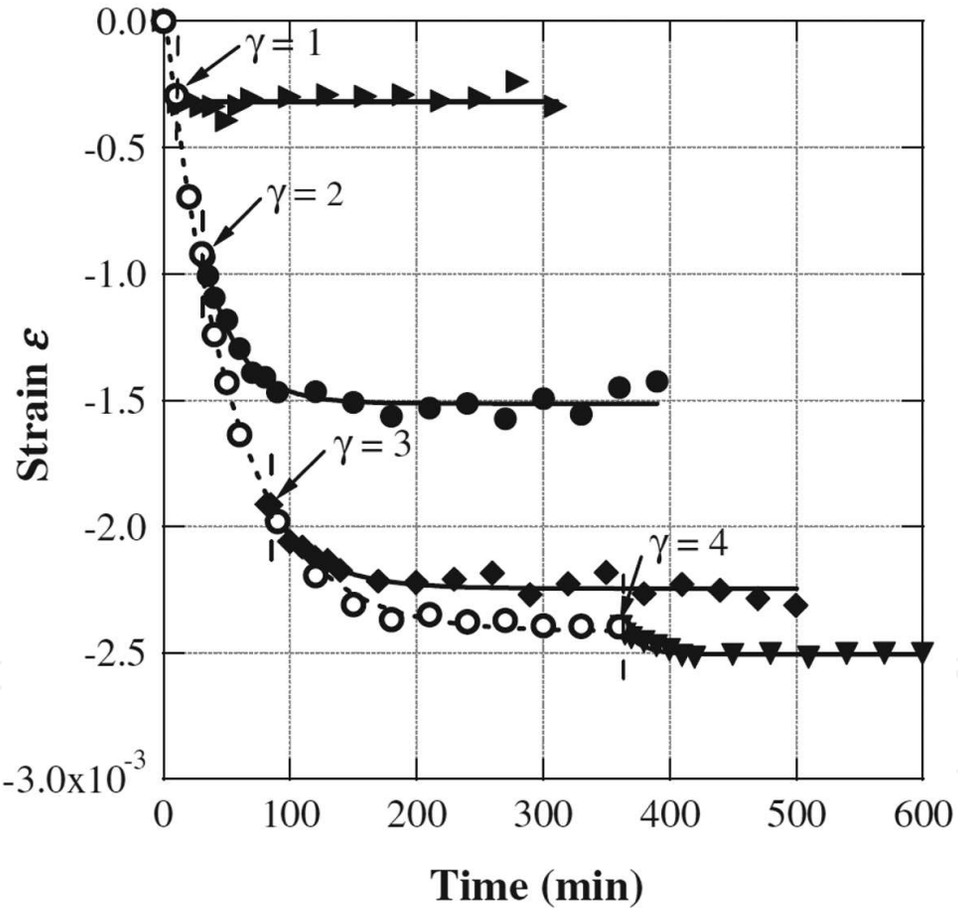

Figure 6. Strain relaxation observed for a PEA sample under curing at different irradiation conditions and the evidence of physical aging phenomena.

reaction was performed taking advantages of the photodimerization of anthracene chemically labeled on the PS chains. The curing reaction was followed by monitoring the change in the absorbance of the photo-cross-linker chemically labeled on PS. It was found that both

the curing kinetics and the deformation induced by the curing reaction can be described by the Kohlrausch-Williams-Watts (KWW) kinetics for kinetically inhomogeneous systems [18]:

$$\gamma(t) = A\left[1-\exp\left\{-k_c\, t\right\}^{\alpha}\right] \tag{17}$$

$$\varepsilon(t) = A\left[1-\exp\left\{-k_d\, t\right\}^{\beta}\right] \tag{18}$$

where A and B are constant, k_c and k_0 are, respectively, rate constant of the reaction and shrinkage. The KWW exponent α and β are less than 1 and in between 0.7 and 0.8.

From the kinetics data expressed by Eqs. (17) and (18), k_d c can be obtained from MZI data and k_c can be deduced from the cross-linking data. It was found that there exists a strong correlation between the curing and the shrinkage processes as illustrated in **Figure 7** [19].

However, the correlation between the cross-link process expressed by the reduced cross-link density $\gamma_r \equiv (\gamma/\gamma_{max})$ and the deformation process indicated by the reduced strain $\varepsilon_r \equiv (\varepsilon/\varepsilon_{max})$ cannot be well expressible by a master curve, particularly at high cross-link density under high light intensity as shown in **Figure 8**. It is worth noting that γ_{max} and ε_{max} are the maximum value at which the cross-link density and the deformation can be achieved at a given light intensity. The increase in the concentration fluctuations in the blends under curing, particularly under high light intensity, would be responsible for the deviation from the master curve.

From the data obtained by MZI, it was also found that the glass transition temperature also plays an important role in the deformation of the cured PS/PVME blends. From the in situ measurements of deformation by MZI under curing, it was found that the photocured sample

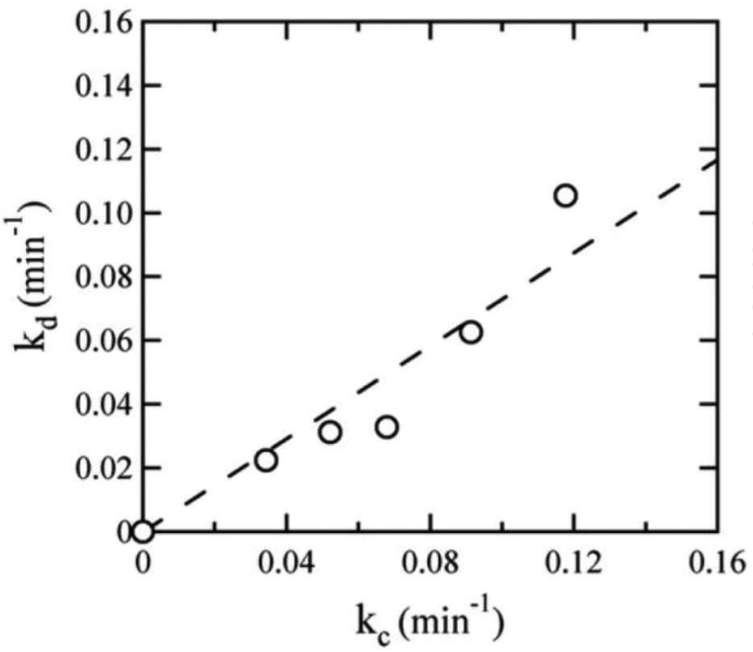

Figure 7. The correlation between the curing reaction kinetics expressed by k c and the deformation process revealed by k d observed for a PS/PVME (30/70) blend.

http://dx.doi.org/10.5772/64611

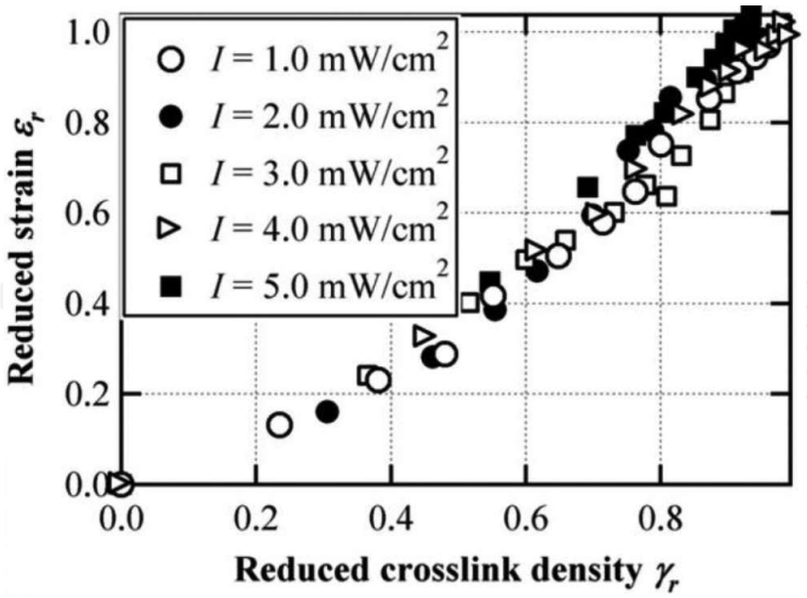

Figure 8. Correlation between the reduced strain and the reduced cross-link density obtained for a PS/PVME (30/70) irradiated with different light intensity ranging from 0.1 to 5.0 mW/cm^2.

undergoes shrinking during the irradiation process, but the sample also partially recovered by swelling back after stopping irradiation. This process is determined by the difference between the experimental temperature and the resulting glass transition temperature T_g of the cured sample at the time of stopping irradiation. This particular swelling behavior was observed upon raising the experimental temperature [19].

3.4. Local deformation observed by MZI in polymer blends undergoing phase separation in the bulk state

So far, Mach-Zehnder interferometry has been utilized to monitor the local deformation in homopolymers and miscible polymer blends under photocuring. For cured polymer mixtures, phase separation took place as the reaction yield exceeds a critical value. The shrinkage induced by curing reaction not only affects the shape of the blend but also influences the phase separation process. For the polymer mixtures with a lower critical solution temperature (LCST) like PS/PVME, cross-linking the PS component will enlarge the unstable region of the mixture and eventually lead to phase separation. The shrinkage of the mixture reveals some unexpected behavior shown in **Figure 9**, as an example, for a PS/PVME (20/80) blend photo-cross-linked by irradiation with 365 nm UV light. Here, the peak of the scattering intensity in situ monitored during the curing process appears and gradually moves toward the side of *wide angle* (*large wavenumber q*), suggesting that the length scale of the bi-continuous structures resulting from the phase separation gradually decreases, instead of increase as in many cases observed for the conventional phase separation process [20]. Taking into account that polymers often undergo shrinkage upon curing, the deformation of a PS/PVME (20/80) blend was in situ monitored by using a Mach-Zehnder interferometry under irradiation with the same conditions. The period ξ of these spinodal structures induced by photocuring was calculated using the Bragg condition $\xi = 2\pi/q_{max}$, where q_{max} is the wavenumber corresponding to the scattering peak of the intensity

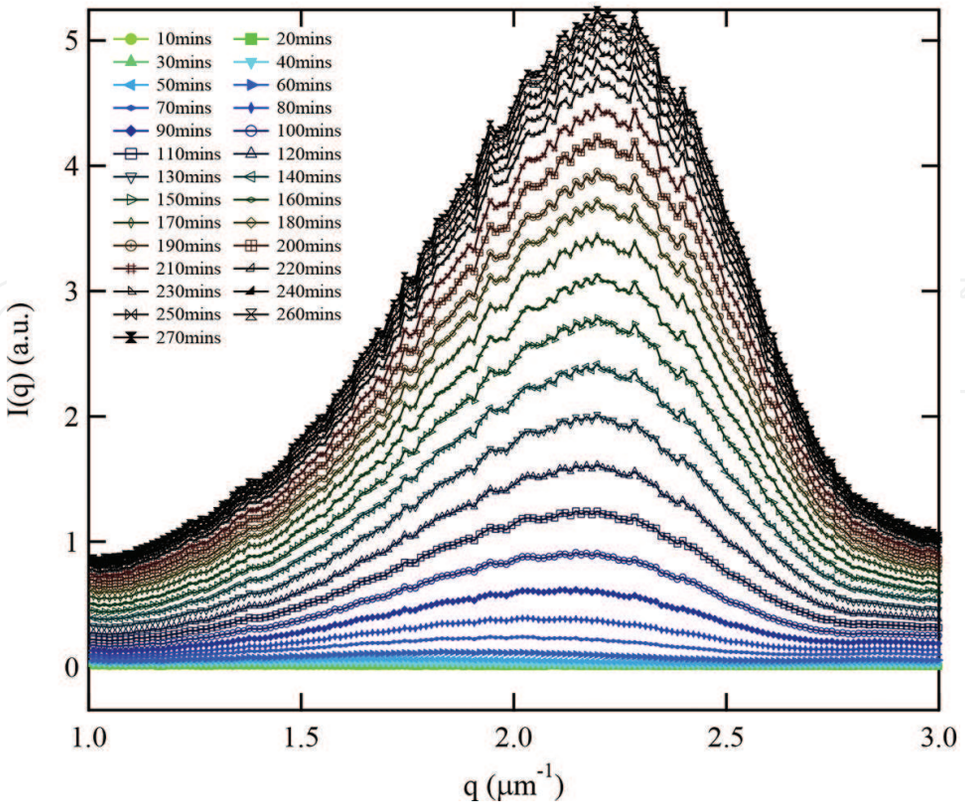

Figure 9. Laser scattering profile obtained for a PS/PVME (20/80) blend photo-cross-link by irradiation with 365 nm UV light. The data were recorded in situ under irradiation. The number in the figure indicates the curing time [21].

distribution shown in **Figure 9**. The plot of the characteristic length scale ξ of the morphology versus the net time of curing clearly shows that ξ decreases with increasing curing (irradiation) time. This result is opposite to the conventional phase separation in the absence of shrinkage, that is, ξ increases as phase separation proceeds. Obviously, as curing time increases, the characteristic length scale gradually decreases and finally reaches a stationary value, indicating the termination of the phase separation process. From the results obtained by Mach-Zehnder interferometry, the elastic strain defined as $(\Delta d/d)$ was calculated and its dependence on curing time was examined. It was found that the elastic strain $(\Delta d/d)$ increases with increasing the irradiation intensity and significantly deviates from these decay curves when phase separation starts. The initial slope of the plot $(\Delta d/d)$ vs. irradiation time, that is $(\tau_i = (\mathrm{d}\ (\Delta d/d\,))/dt)$ can be used as a measure of the characteristic time of shrinkage process induced by the curing reaction. The rate of shrinkage k_i can be defined as $k_i = (1/\tau_i)$. **Figure 10** depicts the clear correlation between the shrinkage obtained from Mach-Zehnder interferometry and the evolution of morphology detected by light scattering, demonstrating again the effectiveness of the Mach-Zehnder interferometry.

A clear correlation was observed between the apparent rate of the phase separation k_ξ obtained from light scattering experiment and the apparent rate of shrinkage k_i obtained from MZI experiments [20]. The results also reveal the significant roles of Mach-Zehnder interferometry in the kinetic studies on polymer phase separation.

http://dx.doi.org/10.5772/64611

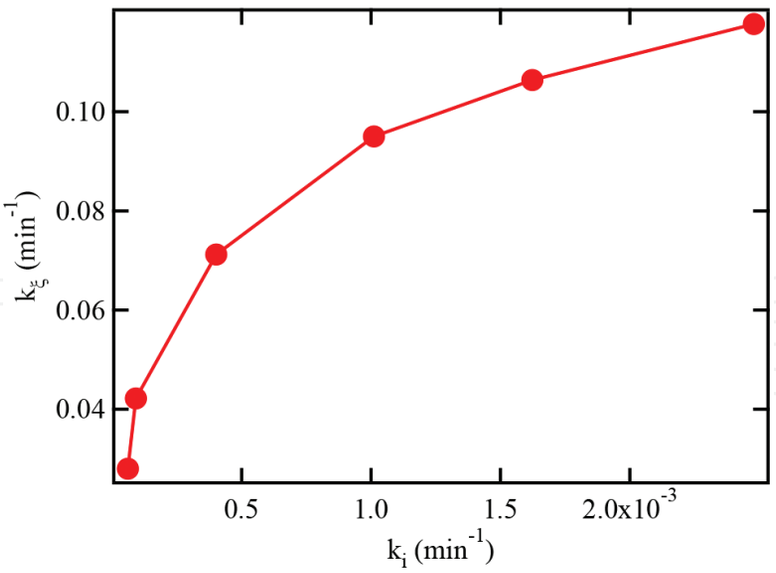

Figure 10. Correlation between the rate of shrinkage caused by photocuring reaction and the apparent rate of phase separation observed for a PS/PVME (20/80) blend photocured with 365 nm UV at 110°C.

Besides the applications of MZI to the polymer researches described above, the effect of polymer molecular weight on the deformation of poly(ethyl acrylate) (PEA) was recently investigated during the photocuring process. The effects of the entanglement molecular weight of PEA on the shrinkage and swelling process were observed by MZI and the results are discussed in terms of polymer diffusion in entangled polymer networks [21].

4. Concluding remarks

For the applications in polymer research, Mach-Zehnder interferometer (MZI) would be a simple instrument to in situ monitor the local deformation in the nanometer scales. The current MZI instrument can be improved in two aspects: accessibility to temperature dependence measurements and improvement of signal-to-noise ratio to increase the data precision. The former requires some careful temperature controls of the experimental environments around the sample and the MZI chamber. On the other hand, the later could be solved by introducing lock-in detection of interference signals. These experiments are underway to prepare for the second generation of Mach-Zehnder interferometry for research on photocuring of polymers.

Acknowledgements

Research described here was financially supported by the Ministry of Education, Japan through Grant-in-Aid for Scientific Research on the Priority-Research-Areas "Molecular NanoDynamics" and "Soft Matter Physics". We greatly appreciate the active participation of

former graduate students at the beginning of the project: Kyosuke Inoue, Satonori Komatsu, Ken Ohdomari and Kazuhiro Sorioka. This experiment would not be successful without their great effort and elaboration.

Author details

Dan-Thuy Van-Pham[1], Minh-Tri Nguyen[1, 2], Hideyuki Nakanishi[1], Tomohisa Norisuye[1] and Qui Tran-Cong-Miyata[1]*

*Address all correspondence to: qui@kit.ac.jp

1 Department of Macromolecular Science and Engineering, Graduate School of Science and Technology, Kyoto Institute of Technology, Kyoto, Japan

2 Department of Chemical Engineering, Can-Tho University, Can-Tho, VietNam

References

[1] Zehnder L: "A new interferometer", (*in German)*. Ein neuer interferenzrefraktor. Zeitschrift fur Instrumentenkunde. 1891, **11**: 275–285.

[2] Mach L: "On an interferometer", (*in German)*. Uber einen interferenzrefraktor. Zeitschrift fur Instrumentenkunde. 1892, **12**: 89–93.

[3] Ji Y, Chung Y, Sprinzak D, Heiblum M, Mahalu D, Shtrikman H: An electronic Mach-Zehnder interferometer. Nature 2003, **422**:415. DOI:10.1038/nature01503.

[4] Goldstein RJ, Kuehn TH. Optical systems for flow measurement: Shadowgraph, Schlieren and interferometric techniques. In: 2nd Goldstein RJ. Fluid Mechanics Measurements. Philadelphia, PA: Taylor & Francis; 1996. 451 p.

[5] Li L, Xia L, Xie Z, Liu D. All-fiber Mach-Zehnder interferometers for sensing applications. Opt. Express 2012, **20**, 11109–11120. DOI: 10.1364/OE.20.011109.

[6] Lapsley M, L, Chiang IK, Zheng YB, Ding XY, Mao X, Huang TJ. A single-layer, planar, optofluidic Mach-Zehnder interferometer for label-free detection. Lab Chip 2011, **11**, 1795–1800. DOI:10 1039/c01c00707b.

[7] Huang Y, Paloczi GT, Yariv A, Zhang C, Dalton LR. Fabrication and replication of polymer integrated optical devices using electron-beam lithography and soft lithography. J. Phys. Chem. B 2004, **108**, 8606–8613. DOI: 10.1021/jp049724d.

[8] Zhao X-M, Smith SP, Waldman SJ, Whitesides GM, Prentiss M: Demonstration of waveguide couplers fabricated using microtransfer molding. Appl. Phys. Lett. 1997, **71**, 1017. DOI: 10.1063/1.119713

[9] Xia Y, Whitesides GM. Soft lithography. Angew. Chem. Intl. Ed. 1998, **37**, 550–575, DOI: 10.1002(SICI)1521-3773(19980316)37:5.

[10] Inoue K, Komatsu S, Trinh XA, Norisuye T, Tran-Cong-Miyata Q. Local deformation in photo-crosslinked polymer blends monitored by Mach-Zehnder interferometry. J. Polym. Sci. Polym. Phys. 2005; **43**, 2898–2913. DOI: 10.1002/polb.20593

[11] Tien PK: Light waves in thin films and integrated optics. Appl. Optics. 1971; **10**, 2395–2413.

[12] Taylor ED, Cates C, Mauel ME, Maurer DA, Nadle D, Navratil GA, Shilov M: Nonstationary signal analysis of magnetic islands in plasmas. Rev. Sci. Instrum. 1999; **70**, 4545–4551. DOI: 10.1063/1.1150110.

[13] Harada A, Tran-Cong Q. Modulated phases observed in reacting polymer mixtures with competing interactions. Macromolecules. 1997, **30**, 1643–1650. DOI: 10.1021/ma961542x

[14] Nakanishi H, Satoh M, Norisuye T, Tran-Cong-Miyata Q. Generation and manipulation of hierarchical morphology in interpenetrating polymer networks by using photochemical reactions. Macromolecules. 2004, **37**, 8495–8498. DOI: 10.1021/ma048657i

[15] Tran-Cong-Miyata Q, Kinohira T, Van-Pham D-T, Hirose A, Norisuye T, Nakanishi H. Phase separation of polymer mixtures driven by photochemical reactions: Complexity and fascination. Curr. Opin. Solid State Mater. Sci. 2011, **15**, 254–261. DOI: 10.1016/j.cossms.2011.06.004

[16] Hutchinson JM. Relaxation processes and physical aging. In: Haward RN, Young RJ, editors. The Physics of Glassy Polymers. London: Chapman & Hall; 1997. pp. 85–153.

[17] Van-Pham D.-T, Sorioka, K, Norisuye T, Tran-Cong-Miyata, Q. Physical aging of photo-crosslinked poly(ethyl acrylate) observed in the nanometer scales by Mach-Zehnder interferometry. Polymer J. 2009, **41**, 260–265. DOI:10.1295/polymj.PJ2008202

[18] Williams G, Watts DC. Non-symmetrical dielectric relaxation behaviour arising from a simple empirical decay function. Trans. Faraday Soc. 1970, **66**, 80–85. DOI: 10.1039/TF9706600080

[19] Van-Pham DT, Sorioka K, Norisuye T, Tran-Cong-Miyata Q. Formation and relaxation of the elastic strain generated by photocuring in polymer blends monitored by Mach-Zehnder interferometry. Polymer 2011, **52**, 739–745. DOI: 10.1016/j.polymer.2010.12.028

[20] Trinh X-A, Fukuda J, Adachi Y, Nakanishi H, Norisuye T, Tran-Cong-Miyata Q. Effects of elastic deformation on phase separation of a polymer blend by a reversible photo-cross-linking reaction. Macromolecules. 2007, **40**, 5566–5574. DOI: 10.1021/ma0705220

[21] Kawamoto T, Van-Pham D-T, Nakanishi H, Norisuye T, Tran-Cong-Miyata Q. Effects of molecular weight on the local deformation of photo-cross-linked polymer blends studied by Mach-Zehnder interferometry. Polymer J. (Tokyo). 2014, **46**, 819–822. DOI:10.1038/pj.2014.63.

IntechOpen